JOURNAL OF BACTERIOLOGY, Aug. 2008, p. 5328–5338 Vol. 190, No. 15
0021-9193/08/$08.00+0 doi:10.1128/JB.00150-08

Identification of the Origin of Transfer (*oriT*) and a New Gene Required for Mobilization of the SXT/R391 Family of Integrating Conjugative Elements[▽]

Daniela Ceccarelli, Aurélie Daccord, Mélissa René, and Vincent Burrus*

Centre d'étude et valorisation de la diversité microbienne (CEVDM), Département de biologie, Université de Sherbrooke, Quebec, Canada

Received 29 January 2008/Accepted 25 May 2008

Integrating conjugative elements (ICEs) are self-transmissible, mobile elements that are widespread among bacteria. Following their excision from the chromosome, ICEs transfer by conjugation, a process initiated by a single-stranded DNA break at a specific locus called the origin of transfer (*oriT*). The SXT/R391 family of ICEs includes SXT^{MO10}, R391, and more than 25 related ICEs found in gammaproteobacteria. A previous study mapped the *oriT* locus of SXT^{MO10} to a 550-bp intergenic region between *traD* and s043. We suspected that this was not the correct *oriT* locus, because the identical *traD*-s043 region in R391 and other SXT/R391 family ICEs was annotated as a gene of an unknown function. Here, we investigated the location and structure of the *oriT* locus in the ICEs of the SXT/R391 family and demonstrated that *oriT*$_{SXT}$ corresponds to a 299-bp sequence that contains multiple imperfect direct and inverted repeats and is located in the intergenic region between s003 and *rumB′*. The *oriT*$_{SXT}$ locus is well conserved among SXT/R391 ICEs, like R391, R997, and pMERPH, and cross-recognition of *oriT*$_{SXT}$ and *oriT*$_{R391}$ by R391 and SXT^{MO10} was demonstrated. Furthermore, we identified a previously unannotated gene, *mobI*, located immediately downstream from *oriT*$_{SXT}$, which proved to be essential for SXT^{MO10} transfer and SXT^{MO10}-mediated chromosomal DNA mobilization. Deletion of *mobI* did not impair the SXT^{MO10}-dependent transfer of the mobilizable plasmid CloDF13, suggesting that *mobI* has no role in the assembly of the SXT^{MO10} mating pair apparatus. Instead, *mobI* appears to be involved in the recognition of *oriT*$_{SXT}$.

Integrating conjugative elements (ICEs) are a large family of self-transmissible mobile genetic elements that are widespread among bacteria (8, 12). These elements confer a range of properties upon the host bacteria, including resistance to antibiotics and heavy metals, virulence, symbiosis establishment, and alternative metabolic pathways. ICEs are made of a core set of genes ensuring their maintenance, mobility, and regulation (8, 12, 44, 50).

Following their excision from the chromosome of the host cell as a circular intermediate, ICEs transfer by conjugation, using a mechanism similar to that of conjugative plasmids (8, 15, 19, 23, 32, 39). Integration into and excision from the chromosome occur by recombination mediated by an ICE-encoded site-specific recombinase called integrase (Int) (10). Several ICEs are able to mobilize nonconjugative plasmids in *cis* and in *trans* as well as chromosomal DNA in an Hfr-like manner (27).

Conjugative DNA transfer takes place in two key steps: (i) biochemical processing of the DNA molecule for transfer and (ii) assembly of a mating apparatus bridging the donor and recipient cells to allow DNA transfer. Typically conjugative DNA transfer is initiated at a specific *cis*-acting site called the origin of transfer (*oriT*), required for efficient translocation of the DNA to the recipient cell (23, 39). A DNA relaxase encoded by the conjugative element recognizes the *oriT* locus and cleaves one strand within the *oriT* locus at a specific site called *nic*, forming a single-strand DNA break. The relaxase remains covalently attached to the 5′ end of the nicked DNA strand (22) that is translocated into the recipient cell through the mating bridge (34, 43, 51). Within the recipient cell, host enzymes convert the transferred single-stranded DNA into double-stranded DNA that can be recircularized and/or recombined into the recipient chromosome.

In most documented cases, auxiliary proteins of both host and plasmid origins assist the relaxase, allowing the formation of a DNA-protein complex known as the relaxosome (14, 42). Plasmid *oriT*s generally contain features, such as inverted repeats and A tracts, that are located near the plasmid strand cleavage site and form hairpins when in single-stranded form (19).

In contrast to plasmid *oriT*s, little is known about initiation of conjugative transfer of ICEs. To date, the *oriT*s from only two ICEs, Tn*916* from *Enterococcus faecalis* and ICE*Bs1* from *Bacillus subtilis*, have been identified and characterized (30, 31). Like conjugative plasmids, ICEs encode their own relaxases, able to recognize and bind to the *oriT*, and cut at the *nic* site. Auxiliary proteins were also described for Tn*916*, which requires the transposon-encoded integrase, conferring both strand and sequence specificities to the endonucleolytic cleavage activity of the relaxase Orf20 (45).

SXT^{MO10} is a 99.5-kb ICE initially identified in clinical strains of *Vibrio cholerae* O139 from India. It confers resistance to chloramphenicol, streptomycin, sulfamethoxazole, and trimethoprim (49). R391 is an ICE derived from a clinical isolate of *Providencia rettgeri* from South Africa (16), conferring kanamycin and mercury resistance (41). Both genetic studies and

* Corresponding author. Mailing address: Département de biologie, Université de Sherbrooke, 2500 Boulevard de l'Université, Sherbrooke, Québec, Canada J1K 2R1. Phone: (819) 821-8000, ext. 65223. Fax: (819) 821-8049. E-mail: Vincent.Burrus@USherbrooke.ca.

▽ Published ahead of print on 6 June 2008.

DNA sequence analyses revealed that R391 and SXT^{MO10} are functionally and genetically related (4, 6, 26). They share a highly conserved genetic backbone, coding for their regulation, excision/integration, and conjugative transfer (3). Genes specific to each ICE are interspersed in the conserved sequence, and hot spots have been identified as targets for different insertions. SXT^{MO10}, R391, and more than 25 related ICEs (1, 9, 29, 38) were recently grouped within the SXT/R391 family (7); all these ICEs are characterized by a highly conserved integrase, Int$_{SXT}$, and by the ability to integrate into the 5′ end of *prfC*, a nonessential gene involved in the termination of translation (28).

Beaber et al. (4) reported that the DNA-processing region of SXT^{MO10} and R391 encompasses three genes: (i) *traI*, which encodes a putative relaxase; (ii) *traD*, which encodes a putative coupling protein that is part of the mating pore and acts as a receptor for the relaxase attached to the region encoded by the 5′ end of the transferred single-stranded DNA strand; and (iii) s043 (*traJ*), encoding another putative conjugation coupling factor. Deletion of any of these three genes abolished SXT^{MO10} transfer (4, 6). Beaber et al. (4) mapped the *oriT* locus of SXT^{MO10} (*oriT*$_{SXT}$) to a 550-bp intergenic region between *traD* and *traJ*. While no open reading frame (ORF) between *traD* and *traJ* in SXT^{MO10} has been annotated (4), *orf35*, a putative ORF that encodes a protein of unknown function, has been annotated to occur at the same locus in R391, with no evidence for the presence of an *oriT* locus (6). The presence of an ORF in this region of R391 led us to question whether *oriT*$_{SXT}$ had been properly assigned. In the present study, we determined that *oriT*$_{SXT}$ is actually located in the intergenic region between s003 and *rumB′* and characterized the minimal *oriT* regions of several ICEs belonging to the family SXT/R391. We also identified a new gene, *mobI*, which is required for SXT^{MO10} transfer as well as for *cis*-mobilization of chromosomal DNA in an Hfr-like manner but not for *trans*-mobilization of the broad-host-range mobilizable plasmid CloDF13.

MATERIALS AND METHODS

Bacterial strains and media. The bacterial strains used in this study are described in Table 1. The strains were routinely grown in Luria-Bertani (LB) broth at 37°C in an orbital shaker/incubator and were maintained at −80°C in LB broth containing 15% (vol/vol) glycerol. Antibiotics were used at the following concentrations: ampicillin (Ap), 100 μg/ml; chloramphenicol, 20 μg/ml; kanamycin, 50 μg/ml; nalidixic acid (Nx), 40 μg/ml; rifampin (Rf), 100 μg/ml; spectinomycin, 50 μg/ml; streptomycin (Sm), 50 μg/ml; sulfamethoxazole (Su), 160 μg/ml; tetracycline (Tc), 12 μg/ml; and trimethoprim (Tm), 32 μg/ml.

Bacterial conjugation. Conjugation assays were used to transfer SXT^{MO10}, R391, or plasmids into *Escherichia coli* strains. Mating assays were performed by mixing equal volumes of overnight cultures of donor and recipient strains. The cells were harvested by centrifugation and resuspended in a 1/20 volume of LB broth. Cell suspensions were poured onto LB agar plates and incubated at 37°C for 6 h. The cells were then resuspended in 1 ml of LB medium, and serial dilutions were plated onto appropriate selective media to determine the numbers of donors, recipients, and exconjugants. Frequency of transfer was expressed as the number of exconjugant cells per donor cell in the mating mixture at the time of plating. Nx- or Rf-resistant derivative strains of *E. coli* MG1655 (VB111 and VB112, respectively) were used as recipients in conjugation experiments. To induce expression of pMobI-B or pMobI-D in complementation assays, mating experiments were carried out with LB agar plates supplemented with 0.02% arabinose.

Plasmid and strain construction. The plasmids used in this study are described in Table 1. Plasmid pACYC184 Δ*cat* was constructed by digestion with MscI/PvuII of pACYC184 DNA harvested from the *dam dcm* strain *E. coli* ER2925 (New England Biolabs). After digestion, the 2,424-bp fragment was religated using T4 DNA ligase (New England Biolabs). All of the pACYC184 Δ*cat*-derived plasmids that were used in mobilization experiments were constructed by cloning of XbaI-flanked PCR products into the XbaI site. Plasmids pMRA, pMRB, pMRC, pMRD, and pMRE were created using the primer pairs MELR1/

TABLE 1. *E. coli* K-12-derivative strains and plasmids used in this study

Strain or plasmid	Relevant genotype or phenotype	Reference or source
Strains		
CAG18439	MG1655 *lacZU118 lacI42*::Tn*10* (Tc^r)	46
CAG18420	MG1655 *lacZU118 lacI42*::Tn*10kan* (Kn^r)	46
VB111	MG1655 Nx^r	This study
VB112	MG1655 Rf^r	This study
HW220	CAG18439 *prfC*::SXT^{MO10} (Cm^r Sm^r Su^r Tm^r Tc^r)	28
VB4	CAG18439 *prfC*::SXT^{MO10} Δ*int*	V. Burrus, unpublished results
VB82	CAG18420 *prfC*::SXT^{MO10} (Cm^r Sm^r Su^r Tm^r Kn^r)	This study
VB95	CAG18420 *prfC*::SXT^{MO10} Δ*int*	This study
VB154	CAG18420 *prfC*::SXT^{MO10} Δ*mobI*	This study
DC5	VB111 *prfC*::SXT^{MO10} (Cm^r Sm^r Su^r Tm^r Nx^r)	This study
DC16	VB111 *prfC*::SXT^{MO10} Δ*oriT*$_1$	This study
DC17	VB111 *prfC*::SXT^{MO10} Δ*oriT*$_2$	This study
DC6	VB111 *prfC*::R391 (Kn^r Nx^r)	This study
DC59	VB111 *prfC*::R391 Δ*oriT*$_1$	This study
DC60	VB111 *prfC*::R391 Δ*oriT*$_2$	This study
Plasmids		
pACYC184	Tc^r Cm^r	New England Biolabs
pSU4628	CloDF13::Tn*A*ΔEcoRV (Ap^r)	13
pACYC184 Δ*cat*	pACYC184 Δ*cat* (ΔMscI-PvuII; Tc^r)	This study
pMRA	pACYC184 Δ*cat* s003-*rumB′* (1,141-bp fragment)	This study
pMRB	pACYC184 Δ*cat rumA*-s024 (829-bp fragment)	This study
pMRC	pACYC184 Δ*cat traD-traJ* (690-bp fragment)	This study
pMRD	pACYC184 Δ*cat traA*-s052 (581-bp fragment)	This study
pMRE	pACYC184 Δ*cat* s071-s072 (579-bp fragment)	This study
pMRA-LM	pACYC184 Δ*cat oriT*$_{SXT}$ (LM fragment)	This study
pMRA-M	pACYC184 Δ*cat oriT*$_{SXT}$	This study
pMRA-MR	pACYC184 Δ*cat oriT*$_{SXT}$-*mobI*	This study
pMRA-Ra	pACYC184 Δ*cat mobI* (first TTG)	This study
pMRA-Rb	pACYC184 Δ*cat mobI* (second TTG)	This study
pDC-oR391	pACYC184 Δ*cat oriT*$_{R391}$	This study
pDC-oR997	pACYC184 Δ*cat oriT*$_{R997}$	This study
pDC-oMERPH	pACYC184 Δ*cat oriT*$_{pMERPH}$	This study
pMobI-B	pBAD-TOPO *mobI* (first TTG codon)	This study
pMobI-D	pBAD-TOPO *mobI* (second TTG codon)	This study
pVI36	pKD13 Δ*kan*::*aad7* (Sp^r) PCR template for one-step chromosomal gene inactivation	17; V. Burrus, unpublished results

TABLE 2. DNA sequences and positions in SXT^{MO10} of the primers used in this study

Primer name	Nucleotide sequence (5′ to 3′)[a]	Positions (GenBank accession no. AY055428)	Use in this study
MELR1	CGCTCTAGAATACGATCCGCAGGA	3199–3220	Cloning of the intergenic region s003-*rumB′*
MELR2	TGCTCTAGAAGGTACGAAGAAAGATTG	3311–3336	Cloning of the intergenic region s003-*rumB′*
MELR3	CCTCTAGAAACACGTTCCATGAACA	24143–24167	Cloning of the intergenic region *rumA*-s004
MELR4	GTTTCTAGAATACGCTCCATGCAATCT	24945–24969	Cloning of the intergenic region *rumA*-s004
MELR5	AGCTCTAGACAGGCAGTATAAGGA	49176–49198	Cloning of the intergenic region *traD-traJ*
MELR6	TTCTCTAGACTAATGACCCGACCACTCCA	49842–49864	Cloning of the intergenic region *traD-traJ*
MELR7	GTCTCTAGAATACGCCAACAGTGCTTG	55176–55201	Cloning of the intergenic region *traA*-s052
MELR8	TGATCTAGAACGCCCAATTGCACA	55732–55754	Cloning of the intergenic region *traA*-s052
MELR9	ACTTCTAGATATTCGAACGCTTGA	80654–80676	Cloning of the intergenic region s071-s072
MELR10	AATTCTAGAAGCCATTGGTCGTTAA	81208–81231	Cloning of the intergenic region s071-s072
oriT1F	GCTCTAGAGGTTTTCAATCAATCAACCG	3347–3370	See Fig. 3A
oriT1R	TTTCTAGAAAACCAATTTCCCCA	3792–3814	See Fig. 3A
oriT2F	GCTCTAGATGGCGGCGGATGA	3516–3536	See Fig. 3A
orfX1F	TTATCTAGATGGGGAAATTGGTTTGG	3785–3810	See Fig. 3A
orfX2F	GGTTCTAGATTTTGGGGTTAATTGGA	3768–3793	See Fig. 3A
orfX-F1d	TGATAGGGGGTTAATTGGAT	3775–3795	Complementation of Δ*mobI* with orfX-R (short ORF)
orfX-F2d	TGATAGGGGAAATTGGTTTG	3790–3810	Complementation of Δ*mobI* with orfX-R (long ORF)
orfX-R	GAAGTAGCGCAGTTGACTGA	4250–4230	
orfXWF	TTTGGCTTTTGGGGTTAATTGGATGGGGAAAT TGGT GTGTAGGCTGGAGCTGCTTCG	3771–3802	Deletion of *mobI* in SXT^{MO10}
orfXWR	GGGACCAGTTACCACGAGTGAAGTAGCGCAG TTGA CATTCCGGGGATCCGTCGACC	4269–4233	Deletion of *mobI* in SXT^{MO10}
DAN1-F	AGGCTCTGTTTGGCGGCGGATGACCTAGTCAAAAAA GTGTAGGCTGGAGCTGCTTCG	3516–3553	Deletion of $oriT_1$ and $oriT_2$ in SXT^{MO10}
DAN1-R	CCCATCCAATTAACCCCAAAAGCCAAAACCACTATC ATTCCGGGGATCCGTCGACC	3762–3798	Used with DAN1-F for deletion of $oriT_2$ in SXT^{MO10}
DAN1-R2	TGCCGTAACAATCACTGTTTGGCGTCTCGATATAAA ATTCCGGGGATCCGTCGACC	3690–3726	Used with DAN1-F for deletion of $oriT_1$ in SXT^{MO10}
DAN2-F	AGGCTCTGTTTGGCGGTGGATGACTGAGCCAAAAAA GTGTAGGCTGGAGCTGCTTCG	5426–5463	Deletion of $oriT_1$ and $oriT_2$ in R391
DAN2-R	CCCATCCAATTAACCCCAAAAACCAAAACTACTATCA TTCCGGGGATCCGTCGACC	5708–5672	Used with DAN1-F for deletion of $oriT_2$ in R391
DAN2-R2	TGCCGTAACAATCACTGTTTGGCGTCTCGATATAAA ATTCCGGGGATCCGTCGACC	5636–5600	Used with DAN2-F for deletion of $oriT_1$ in R391

[a] Underlined nucleotides indicate the XbaI site introduced for cloning purposes.

MELR2, MELR3/MELR4, MELR5/MELR6, MELR7/MELR8, and MELR9/MELR10, respectively, and genomic DNA of *E. coli* HW220 as a template (Tables 1 and 2). Plasmids pMRA-LM, pMRA-M, pMRA-MR, pMRA-Ra, and pMRA-Rb were constructed using the primer pairs oriT1F/oriT1R, oriT2F/oriT1R, oriT2F/MELR2, orfX2F/MELR2, and orfX1F/MELR2, respectively, and genomic DNA of *E. coli* HW220 as a template (Tables 1 and 2). pDC-oR391, pDC-oR997, and pDC-oMERPH were constructed using the primer pair oriT2F/oriT1R and genomic DNA of *E. coli* DC6, AB1157 R997, and AB1157 pMERPH (36), respectively, as templates. PCR products were purified from a 1% agarose gel by using a QIAquick gel extraction kit (Qiagen), digested by XbaI, and ligated to XbaI-digested DNA of pACYC184 Δ*cat*, using T4 DNA ligase (New England Biolabs). The inserts of pMRA and all the pACYC184 Δ*cat*-derivative plasmids containing fragments that overlap the s003-*rumB′* intergenic region were in the same orientation. Plasmids pMobI-D and pMobI-B, used for complementation assays, were constructed by cloning the short (426-bp) or long (444-bp) version of *mobI*. The gene *mobI* was amplified by PCR using primer pair orfX-F1d/orfX-R or orfX-F2d/orfX-R, respectively, into the TA cloning expression vector pBAD-TOPO (Invitrogen) according to the manufacturer's instructions.

Δ*mobI*, Δ$oriT_1$, and Δ$oriT_2$ mutations were introduced into SXT^{MO10} by using the one-step chromosomal gene inactivation technique (17) with primers orfXWF/orfXWR, DAN1-F/DAN1-R2, and DAN1-F/DAN1-R, respectively, and pVI36 as the template (Tables 1 and 2) as previously described (4). Similarly, Δ$oriT_1$ and Δ$oriT_2$ mutations were introduced into R391 by using the same technique with primers and DAN2-F/DAN2-R2 and DAN2-F/DAN2-R, respectively, and pVI36 as the template.

Molecular biology techniques. Plasmid DNA was prepared with a QIAprep spin mini prep kit (Qiagen) or a QIAfilter plasmid midi kit (Qiagen), as described in the manufacturer's instructions. All the enzymes used in this study were provided by New England Biolabs and were used according to manufacturer's instructions. The PCR assays for amplifying fragments cloned into the pACYC184 Δ*cat* vector were performed with the primers described in Table 2 with 50-μl PCR mixtures with 1 U of *Taq* DNA polymerase (New England Biolabs). The PCR conditions were as follows: (i) 3 min at 94°C; (ii) 30 cycles of 30 s at 94°C, 30 s at a suitable annealing temperature, and 30 s to 90 s at 72°C; and (iii) 2 min at 72°C. When needed, PCR products were purified using a QIAquick PCR purification kit (Qiagen) according to the manufacturer's instructions. The purified PCR products or inserts of constructed plasmids were sequenced by DNA LandMarks, Inc. (Saint-Jean-sur-Richelieu, Quebec, Canada). The DNA sequences were compared with the GenBank DNA sequence database by using the BLASTN program (2). *E. coli* was transformed by electroporation according to Dower et al. (18), using a Bio-Rad GenePulser Xcell apparatus set at 25 μF, 200 Ω, and 2.5 kV.

RESULTS

Location of $oriT_{SXT}$ revisited. To characterize further the 550-bp region of SXT^{MO10} that was reported as containing *oriT* (4) and determine the minimal segment required for efficient transfer, we amplified by PCR a 690-bp fragment overlapping

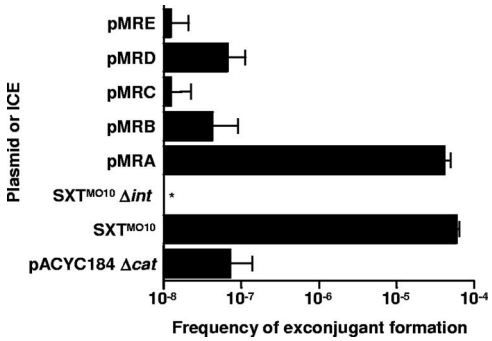

FIG. 1. Identification of the *cis*-acting region of SXT^{MO10} required for efficient transfer of a nonmobilizable vector. Mobilization of plasmids containing various intergenic regions of SXT^{MO10} was assessed using a conjugation assay. The inserts in these plasmids, all derivatives of the nonmobilizable vector pACYC184 Δ*cat*, were intergenic regions s003-*rumB′* (pMRA), *rumA*-s024 (pMRB), *traD-traJ* (pMRC), *traA*-s052 (pMRD), and s071-s072 (pMRE). The frequency of exconjugant formation was obtained by dividing the number of exconjugants (Tc^r Nx^r CFU) by the number of donors (Kn^r CFU). Mobilization assays were carried out using *E. coli* CAG18420 SXT^{MO10} Δ*int* (VB95) as the donor strain. The frequency of transfer of SXT^{MO10} was determined by using *E. coli* VB82 as a donor strain. *E. coli* VB111, a Nx^r-derivative strain of *E. coli* MG1655 was used as the recipient strain in all the assays. The bars represent the mean and standard deviation values obtained from three independent experiments. The asterisk indicates that the frequency of exconjugant formation was below the limit of detection (1×10^{-8}).

the *traD-traJ* intergenic region and cloned it into pACYC184 Δ*cat*. This plasmid is a Tc resistance-conferring vector derived from the low-copy-number, nonmobilizable plasmid pACYC184. We aimed to use the resulting plasmid, pMRC, as a positive control to compare the efficiency of mobilization by SXT^{MO10} of plasmids harboring a range of shorter fragments overlapping the insert of pMRC.

pMRC was introduced into *E. coli* VB95, a strain that contains a Δ*int* mutant of SXT^{MO10} able to produce the Tra proteins required for conjugative transfer but unable to excise from the chromosome. The use of SXT^{MO10} Δ*int* ensures that mobilization of the plasmid does not occur by homologous recombination-mediated cointegration with and subsequent transfer of SXT^{MO10} to the recipient (Fig. 1). A *recA* strain could not be considered for these experiments, since the presence of *recA* is essential for an adequate expression of the *tra* genes in SXT^{MO10} (5).

VB95 pMRC was used as a donor in mating experiments involving a Nx-resistant derivative of *E. coli* MG1655 as a recipient strain (Fig. 1). Nx^r Tc^r exconjugants normally formed at a very low frequency when pACYC184 Δ*cat* was used as a negative control. Indeed, this plasmid cannot be mobilized unless its insert contains a genuine *oriT* locus that is recognized by the transfer proteins encoded by SXT^{MO10}. Surprisingly, we observed that the frequency of transfer of pMRC was lower than that of the control and more than 3 orders of magnitude lower than that of wild-type SXT^{MO10} (Fig. 1). This observation was in marked contrast with the Beaber et al. report (4) in which the 550-bp *traD-traJ* intergenic region was found to allow the mobilization by SXT^{MO10} of a high-copy-number, nonmobilizable vector at a frequency that was similar to that of SXT^{MO10}. To determine the reason for this discrepancy, we took a closer look at the *traD-traJ* region of SXT^{MO10}.

Our analysis of the sequence of the fragment of SXT^{MO10} (GenBank accession no. AY055428) that encompasses *traD* and *traJ* (positions 45,042 to 51,360) revealed three sequence mismatches and one +1 frameshift mutation compared to the sequence of the same locus (positions 64,662 to 58,345) in the whole genome of *V. cholerae* MO10 (GenBank accession no. NZ_AAKF00000000), i.e., the original host of SXT^{MO10} (data not shown). Resequencing of this region based on PCR products amplified from HW220 (Table 1), an *E. coli* CAG18439 exconjugant containing SXT^{MO10}, revealed 100% identity at the nucleotide level with the sequence of MO10. Taking into account these four sequence alterations in the SXT^{MO10} genome, the *traD-traJ* intergenic region of SXT^{MO10} in *V. cholerae* MO10 actually contains a 561-bp ORF that was overlooked in the previous annotation and codes for an hypothetical protein designated VchoM_02001241 (GenBank accession no. NZ_AAKF02000011, nucleotides 59939 to 60499).

Nucleotide BLAST analysis of VchoM_02001241 against the GenBank database revealed 94% identity with *orf35* of R391 from *P. rettgeri* (AY090559.1) and *orf1755* of ICE*Spu*PO1 from *Shewanella* sp. strain W3-18-1 (CP000503) as well as 95% identity with a hypothetical ORF of ICE*Pda*Spa1 from the fish pathogen *Photobacterium damselae* subsp. *piscicida* (AJ870986). *orf35* and *orf1755* code for hypothetical proteins of unknown functions (6, 40). Our analysis did not reveal any domain or molecular arrangement typical of *oriT*s in VchoM_02001241, *orf35*, *orf1755*, or the hypothetical ORF in ICE*Pda*Spa1.

The presence of an ORF between *traD* and *traJ* and our inability to mobilize pMRC conflicted with previously published data (4) and led us to reconsider the localization of *oriT* in the ICEs of the SXT/R391 family.

***oriT*$_{SXT}$ is located within the intergenic region s003-*rumB′*.** We adopted a comparative genomics approach that facilitated rapid identification of the region of SXT^{MO10} that contained *oriT*. We reasoned that this functional fragment was likely to be (i) an intergenic sequence and (ii) a region conserved in the core set of sequences shared by SXT^{MO10}, R391, and the other ICEs of the SXT/R391 family. We identified four intergenic regions that met these criteria: s003-*rumB′*, *rumA*-s024, *traA*-s052, and s071-s072, here named A, B, D, and E, respectively.

The four intergenic regions were amplified by PCR (see Table 2 for primer details) and cloned into pACYC184 Δ*cat*, yielding the plasmids pMRA, pMRB, pMRD, and pMRE. Each plasmid was introduced into *E. coli* VB95. The results of mating experiments involving *E. coli* VB95 donors harboring each plasmid are shown in Fig. 1. All plasmids but pMRA exhibited transfer frequencies comparable to or below that of the empty vector, i.e., 3 to 4 orders of magnitude below that of SXT^{MO10}. In fact, phenotypic and molecular analysis of apparent Nx^r Tc^r exconjugants indicated that most colonies were spontaneous Nx^r mutants of donor cells and not genuine exconjugants (data not shown), confirming the absence of cotransfer of SXT^{MO10} Δ*int* with the pACYC184 Δ*cat* derivatives. In contrast, pMRA transferred at a rate that was comparable to the rate of transfer of SXT^{MO10} (Fig. 1).

These data demonstrate that *oriT*$_{SXT}$ was located not in the *traD-traJ* region but in the intergenic region between s003 and *rumB′* instead.

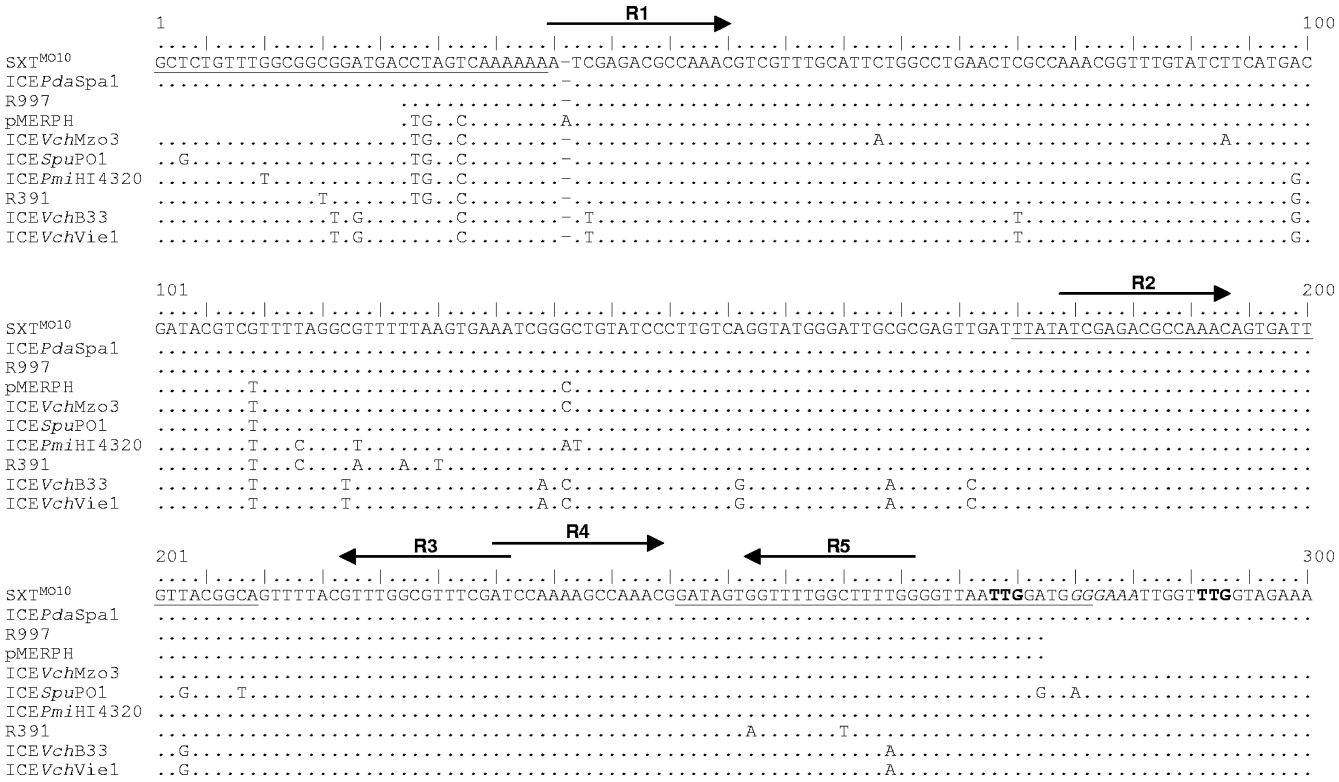

FIG. 2. ClustalW alignment of the 299-bp M fragment located within the s003-*rumB′* intergenic region of SXT^{MO10}, with the corresponding sequences from nine different SXT/R391 ICEs. The SXT^{MO10} sequence from the whole genome of *V. cholerae* MO10 (GenBank accession no. NZ_AAKF00000000) is used as the reference. Identical nucleotides in other ICEs are represented by dots, whereas variations of nucleotide sequence are indicated at the corresponding positions. Underlined nucleotides indicate the positions of primers DAN1-F, DAN1-R2, and DAN1-R, used for $oriT_{SXT}$ deletions. In the same positions are the primers DAN2-F, DAN2-R2, and DAN2-R, used for $oriT_{R391}$ deletions. The imperfect direct and indirect repeats are shown by arrows. The two possible TTG initiation codons of *mobI* are shown in bold. The putative ribosome binding site upstream from the second TTG of *mobI* is shown in italic.

The intergenic region s003-*rumB′* is conserved in SXT/R391 ICEs and contains a new ORF. The 918-bp s003-*rumB′* intergenic region was further analyzed. Nucleotide BLAST analysis revealed that this region shares 95%, 97%, 100%, and 96% identity with corresponding regions of R391 (GenBank accession no. AY090559.1), ICE*Spu*PO1 (GenBank accession no. NC_008750.1), ICE*Pda*Spa1 (GenBank accession no. AJ870986), and the incompletely characterized ICE*Vch*Vie1 from *V. cholerae* V21 (GenBank accession no. AB114188), respectively. This intergenic region also shares 96% identity with segments of the genomes of *V. cholerae* B33 (GenBank accession no. NZ_AAWE01000040), *V. cholerae* MZO-3 (GenBank accession no. NZ_AAUU01000001), and the uropathogenic strain *Proteus mirabilis* HI4320 (GenBank accession no. AM942759). These three strains harbor uncharacterized ICEs of the SXT/R391 family that we named here ICE*Vch*B33, ICE*Vch*MZO3, and ICE*Pmi*HI4320, respectively. A ClustalW alignment of these sequences showed that the intergenic region that contains the SXT^{MO10} *oriT* locus is extremely well conserved among the SXT/R391 ICEs (299 bp of this intergenic region are shown in Fig. 2).

Further analysis of the 918-bp intergenic region s003-*rumB′* revealed the presence of a set of five imperfect direct and inverted repeats located 222 bp upstream from the initiation codon of s003 (Fig. 2). Direct and inverted repeats are a common feature found in *oriT* regions in conjugative plasmids (39). These repeats might be involved in the specific recognition of the *oriT* locus by the relaxase and/or accessory proteins, allowing the single-strand, site-specific cleavage reaction to take place at the *nic* site (21, 24, 39).

An ORF of 444 nucleotides, here named *mobI*, directed toward *rumB′* was identified 13 bp downstream from the *rumB′* stop codon by using the gene prediction program GeneMark.hmm (33) (Fig. 3A). *mobI* was overlooked in the previous annotation of the SXT^{MO10} genome, likely due to its anomalous initiation codon TTG. Two alternative TTG initiation codons were identified at positions 1 and 19 of this ORF, producing two possible translation products of 146 and 140 amino acids, respectively. Protein BLAST analysis (BlastP) of both putative proteins did not reveal any similarity with existing proteins or conserved domains in the GenBank database. However, we found that *mobI* was also present in R391, ICE*Spu*PO1, ICE*Pda*Spa1, ICE*Vch*Vie1, ICE*Vch*B33, ICE*Vch*MZO3, and ICE*Pmi*HI4320. In each ICE, *mobI* contained the two alternative TTG initiation sites and encoded putative proteins that shared between 97 and 100% identity with the two alternative hypothetical proteins encoded by *mobI* in SXT^{MO10}. The conservation of *mobI* suggests that this ORF could play a significant role as a protein-encoding gene in the transfer or maintenance of SXT/R391 ICEs.

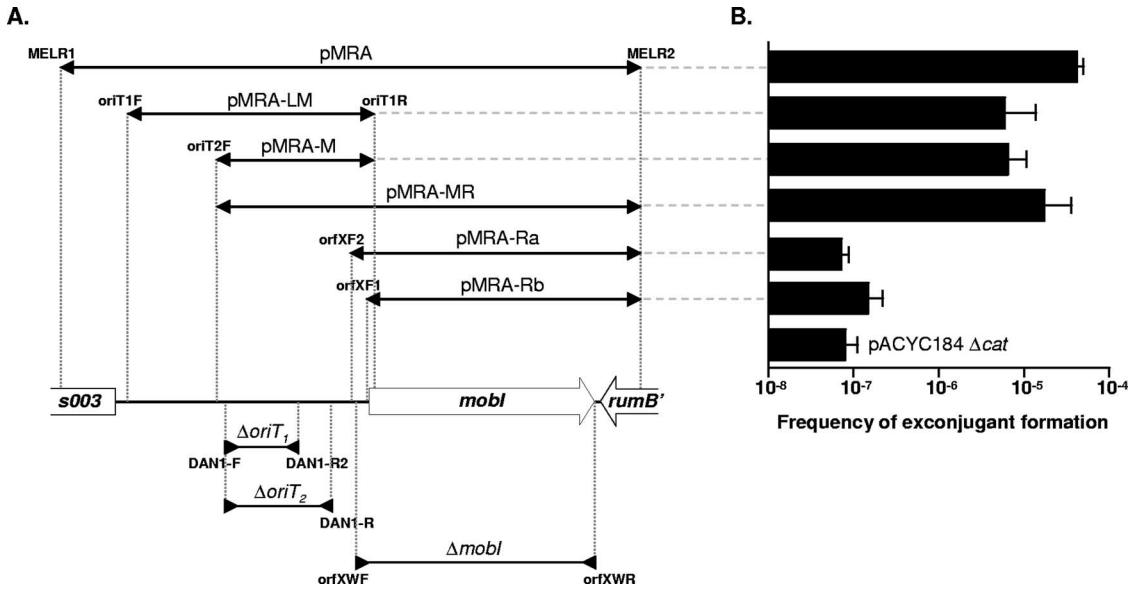

FIG. 3. Identification of the *oriT* locus of SXT^{MO10}. Panel A is a schematic representation of the region of SXT^{MO10} encompassing the beginning of s003 and the end of *rumB′*. The positions of s003, *mobI*, and *rumB′* are indicated. The inserts of the plasmids used in mobilization experiments, all of which were derived from the low-copy-number, nonmobilizable vector pACYC184 Δ*cat*, are represented above the genetic map by overlapping segments delimited by arrows pointing outwards. Deletions within the region are depicted below the genetic map by overlapping segments delimited by arrows pointing inwards. The positions of the oligonucleotides used for amplification and cloning or construction of the deletions are indicated. Panel B corresponds to the results of experiments determining the mobilization of the different plasmids by SXT^{MO10} Δ*int*. The frequency of exconjugant formation was obtained by dividing the number of exconjugants (Rf^r Tc^r CFU) by the number of donors (Kn^r CFU). In all the cases, the donor was *E. coli* VB95 and the recipient strain was *E. coli* VB112. The bars indicate the mean values and standard deviations of results from three independent experiments.

***oriT* is a 299-bp segment located upstream from *mobI*.** To further localize the site of *oriT*$_{SXT}$ within the 918-bp s003-*rumB′* region, five distinct overlapping fragments of 468 bp (LM), 299 bp (M), 821 bp (MR), 550 bp (Rb), and 571 bp (Ra) were amplified by PCR and cloned into pACYC184 Δ*cat*, yielding pMRA-LM, pMRA-M, pMRA-MR, pMRA-Ra, and pMRA-Rb, respectively (Fig. 3A). Inserts Ra and Rb both contain *mobI* and differ only by the forward primers used to amplify the region, containing the first and the second TTG initiation codons of *mobI*, respectively. Insert M contains the DNA sequence overlapping the five imperfect direct and inverted repeats described above. The five resulting plasmids were introduced into *E. coli* VB95, and mobilization assays were carried out as described above. The results of these experiments are shown in Fig. 3B.

The frequency of exconjugant formation for the plasmids containing insert Ra or Rb did not differ significantly from that of the empty vector. This result indicates that neither of these two inserts contained *oriT*$_{SXT}$ as they were not mobilized by SXT^{MO10} Δ*int*. Therefore, *mobI* does not correspond to the functional *cis*-acting *oriT* locus. In marked contrast, all of the plasmids harboring inserts overlapping the segment M, such as LM and MR, were found to be mobilizable by SXT^{MO10} Δ*int*. In addition, insert M itself was sufficient to allow SXT^{MO10} Δ*int*-mediated mobilization of the plasmid, suggesting that *oriT*$_{SXT}$ was located within this 299-bp fragment. Interestingly, the frequency of exconjugant formation for pMRA-LM and pMRA-M was slightly lower than that of pMRA (Fig. 3B). Such a reduction of the frequency of transfer might result from missing *cis*-acting auxiliary sequences that could enhance the efficiency of transfer. Indeed, the presence of *mobI* on the plasmid seemed to slightly increase the efficiency of transfer as shown in Fig. 3B.

In an attempt to narrow the size of the functional *oriT*$_{SXT}$ sequence, we constructed two deletion mutants in the 299-bp M region. In the first mutant, SXT^{MO10} Δ*oriT*$_1$ (DC16), a 139-bp segment containing the repeated sequence R1 was deleted (Fig. 2 and 3A). In the second mutant, SXT^{MO10} Δ*oriT*$_2$ (DC17), a 211-bp segment including the repeated sequences R1 to R4 was deleted. Both deletions were designed to avoid affecting the first putative initiation codon of *mobI* (Fig. 2 and 3A). *E. coli* DC16 and DC17 were used as donor strains in mating assays to assess the effect of each deletion on SXT^{MO10} transfer. Both mutations had a marked effect: the Δ*oriT*$_1$ mutation decreased 120-fold the rates of transfer of the Su and Tm markers compared to the wild type, whereas the Δ*oriT*$_2$ mutation nearly abolished the transfers of these two markers (Fig. 4).

We also constructed the same 139-bp Δ*oriT*$_1$ and 211-bp Δ*oriT*$_2$ mutations in R391 as in SXT^{MO10}, assuming that *oriT*$_{R391}$ was located at the same locus as in SXT^{MO10} and that these deletions would affect R391 transfer as they did for SXT^{MO10}. Indeed, while the overall rate of transfer of R391 was about 10-fold higher than that of SXT^{MO10}, as observed for SXT^{MO10}, the deletion mutants R391 Δ*oriT*$_1$ (DC59) and R391 Δ*oriT*$_2$ (DC60) exhibited low frequencies of transfer compared to the wild type: the Δ*oriT*$_1$ mutation strongly decreased the rate of transfer of the Kn marker, and the Δ*oriT*$_2$ mutation nearly abolished it (Fig. 4).

These data clearly indicated that the region overlapping the

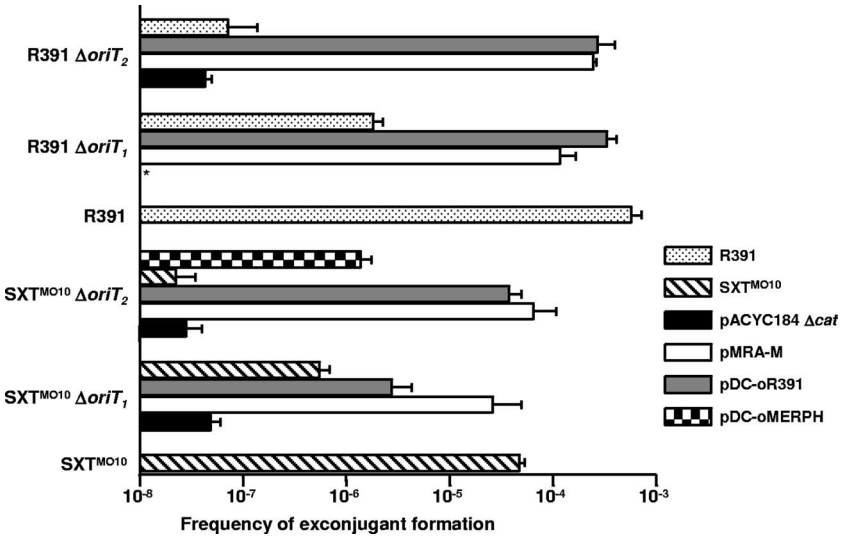

FIG. 4. Cross-recognition and activity of SXT^{MO10} and R391 on their cognate *oriT*s and on the *oriT* locus of pMERPH. The plasmids used in mobilization experiments, all of which were derived from the low-copy-number, nonmobilizable vector pACYC184 Δ*cat*, contained the *oriT* fragment from SXT^{MO10} (pMRA-M), R391 (pDC-oR391), or pMERPH (pDC-oMERPH). pACYC184 Δ*cat* was used as a negative control. All donors were derivatives of *E. coli* VB111 containing SXT^{MO10} or R391 or the $\Delta oriT_1$ or $\Delta oriT_2$ mutants of these two ICEs. In all the cases, the recipient strain was *E. coli* VB112. Frequency of exconjugant formation was determined by dividing the number of exconjugants (Rf^r Tc^r CFU for the pACYC184 Δ*cat* derivatives, Rf^r Kn^r CFU for R391 mutants, or Rf^r Su^r Tm^r CFU for SXT^{MO10} mutants) by the number of donors (Nx^r CFU). The bars indicate the mean values and standard deviations of results from three independent experiments. The asterisk indicates that the frequency of exconjugant formation was below the limit of detection (1×10^{-8}).

repeats R1 to R4, absent in the $\Delta oriT_2$ mutants, was necessary for efficient transfer of both SXT^{MO10} and R391. Interestingly, while deletion of the first 139 bp starting at the repeat R1 strongly affected the transfer of both SXT^{MO10} and R391, it did not completely abolish it.

Cross-recognition of different *oriT* alleles between the members of the SXT/R391 family. Although the alignment of *oriT* sequences of the ICEs of the SXT/R391 family revealed that this region is highly conserved (Fig. 2), differences exist. R391 is one of the ICEs that exhibit the highest divergence in this particular segment. Furthermore, while all the Tra proteins that are encoded by SXT^{MO10} and R391 share from 98 to 100% identity, $TraI_{SXT}$, the putative relaxase encoded by SXT^{MO10}, is only 94.3% identical to $TraI_{R391}$, the putative relaxase encoded by R391. We wondered whether this divergence could confer specificity to the relaxase for the recognition of its cognate *oriT* locus; for instance, $TraI_{R391}$ might not recognize or act at $oriT_{SXT}$ as efficiently as $oriT_{R391}$ and vice and versa.

To assess whether this divergence was conferring to SXT^{MO10} and R391 any specificity for their cognate *oriT* loci, we compared the rate of mobilization by each ICE of plasmids containing one or the other *oriT*. First, the 299-bp M fragment of R391 was amplified by PCR and cloned into pACYC184 Δ*cat*, giving pDC-oR391. We verified that pDC-oR391 was mobilizable by R391 by introducing it into and mobilizing it from *E. coli* DC59 and DC60, two strains containing, respectively, R391 $\Delta oriT_1$ and R391 $\Delta oriT_2$ to avoid cointegration and cotransfer of pDC-oR391 with R391. As shown in Fig. 4, pDC-oR391 was mobilized by both mutants at a frequency that was comparable to that of wild-type R391, clearly demonstrating the presence of $oriT_{R391}$ in the insert of this plasmid.

We then investigated the specificity of SXT^{MO10} and R391 for their cognate *oriT* loci by comparing the frequencies of mobilization of pMRA-M ($oriT_{SXT}$) and pDC-oR391 ($oriT_{R391}$) from *E. coli* VB111 harboring Δ*oriT* mutants of either SXT^{MO10} or R391. We found that SXT^{MO10} $\Delta oriT_1$ and SXT^{MO10} $\Delta oriT_2$ were able to mobilize both pMRA-M and pDC-oR391 at comparable rates (Fig. 4); yet, SXT^{MO10} $\Delta oriT_1$ mobilized pMRA-M slightly more efficiently than pDC-oR391. Similar results were observed with R391 $\Delta oriT_1$ and R391 $\Delta oriT_2$ for both plasmids, but without any significant difference with either of these two plasmids.

We extended our study to the *oriT* loci of two other ICEs belonging to the SXT/R391 family: R997 from *Proteus mirabilis* and pMERPH from *Shewanella putrefaciens*. Since the complete sequences of these two ICEs were not available, we amplified the 299-bp M region by using the same primer pair as for amplification of $oriT_{SXT}$ and $oriT_{R391}$ (Table 2). The amplicons were cloned into pACYC184 Δ*cat*, yielding plasmids pDC-oR997 and pDC-oMERPH, and sequenced (Fig. 2). Interestingly, ClustalW alignment of the cloned fragment revealed that the regions encompassing *oriT* are virtually identical in SXT^{MO10}, ICE*Pda*Spa1, and R997. Since $oriT_{R997}$ and $oriT_{SXT}$ are identical and mobilization of pDC-oR997 ($oriT_{R997}$) was expected to yield results identical to that of pMRA-M, only mobilization of pDC-oMERPH ($oriT_{pMERPH}$) was carried out (Fig. 4). We observed that SXT^{MO10} $\Delta oriT_2$ was able to mobilize the plasmid containing $oriT_{pMERPH}$ to the recipient. However, the rate of transfer of pDC-oMERPH was more than 10 times lower that the rate of transfer of pMRA-M. This defect could be attributed to the insertion of a single nucleotide into the R1 repeat in pDC-oMERPH (Fig. 2). This hypothesis is consistent with the observation that the absence of the repeat R1 in the

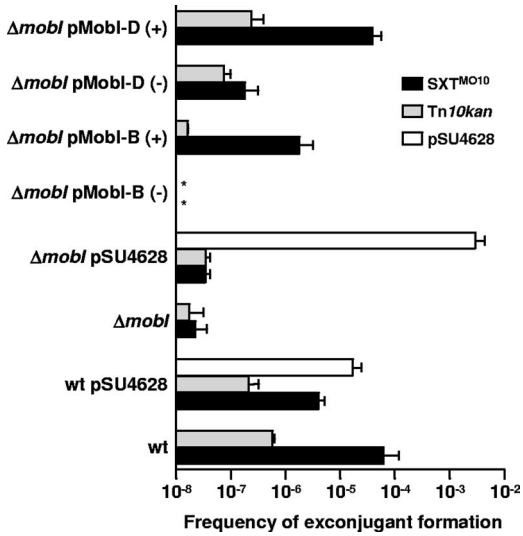

FIG. 5. Role of *mobI* in conjugative transfer of SXT^{MO10} and mobilization of chromosomal DNA or of a broad-host-range mobilizable plasmid. The donors were either *E. coli* VB154, which harbors SXT^{MO10} Δ*mobI* (Δ*mobI*), or *E. coli* VB82, which contains SXT^{MO10} (wt), and the recipient strain was *E. coli* VB112. When indicated, the donor strains also harbored pSU4628, a derivative of the mobilizable plasmid CloDF13, or pMobI-D or pMobI-B, which contained, respectively, the short (426-bp) or the long (444-bp) version of *mobI* under the control of the arabinose-inducible promoter P_{BAD}. (+) and (−) indicate the presence or absence of arabinose during mating for induction of *mobI* expression. The frequencies of exconjugant formation were determined by dividing the number of exconjugants (Rf^r Su^r Tm^r CFU for SXT^{MO10} Δ*mobI*, Rf^r Kn^r CFU for *lacI42*::Tn*10kan*, or Rf^r Ap^r CFU for pSU4628) by the number of donors (Kn^r CFU). The bars show the mean and standard deviation values obtained from three independent experiments. The asterisk indicates that the frequency of exconjugant formation was below the limit of detection (1×10^{-8}).

Δ$oriT_1$ mutants strongly diminishes the transfers of both SXT^{MO10} and R391.

Together, these data indicate that the divergences observed among the members of the SXT/R391 family, between the TraI proteins, and between the *oriT* loci do not seem to constitute a barrier to the initiation of transfer at the *oriT* locus of another ICE of the SXT/R391 family.

***mobI* is required for SXT^{MO10} transfer and acts in *trans*.** To investigate the role of *mobI* in the transfer of SXT^{MO10}, we constructed the deletion mutant *E. coli* CAG18420 SXT^{MO10} Δ*mobI* (VB154). The frequency of transfer of SXT^{MO10} Δ*mobI* from CAG18420 was more than 3 orders of magnitude lower than that of wild-type SXT^{MO10} (Fig. 5). This observation indicated that *mobI* is necessary for efficient transfer of SXT^{MO10} by conjugation. Moreover, the necessity of *mobI* for efficient transfer of $oriT_{SXT}$ from VB154 was confirmed in pMRA-M mobilization assays. Very few Rf^r Tc^r exconjugants (4.5×10^{-8}) could be recovered from a mating experiment involving VB154 pMRA-M as a donor strain and *E. coli* VB112 as a recipient strain, indicating that, unlike wild-type SXT^{MO10}, SXT^{MO10} Δ*mobI* is not able to mobilize a plasmid harboring $oriT_{SXT}$.

Complementation analyses demonstrated that *mobI* acts in *trans* and confirmed that it is not part of the *cis*-acting *oriT* locus. As shown in Fig. 5, introduction into VB154 of pMobI-D or pMobI-B, two plasmids containing the short (426-bp) or long (444-bp) version of *mobI* under the control of P_{BAD}, restored the transfer of SXT^{MO10} Δ*mobI* in the presence of arabinose. In contrast, in the absence of arabinose, very little or no complementation was observed. Interestingly, the 426-bp *mobI* sequence was sufficient to complement the transfer defect of SXT^{MO10} Δ*mobI*, suggesting that the second TTG codon is the genuine start codon for *mobI*. pMobI-B was unable to restore the transfer of SXT^{MO10} Δ*mobI* to the wild-type level, suggesting that the distance between the P_{BAD} promoter and the second initiation codon of *mobI* was not ideal in the long version of the gene. This hypothesis is also supported by the presence of a suitable ribosome binding site (GGGAAA), located 5 bp upstream from the second TTG initiation codon. In ICE*Spu*PO1, this sequence is even closer to the consensus ribosome binding site motif (AGGAAA) (Fig. 2). No such translation initiation signal can be found upstream from the first TTG codon of *mobI*. Together, these findings indicate that *mobI* is a *trans*-acting gene required for the conjugative transfer of SXT^{MO10}; it is likely that *mobI* is also required for transfer of all ICEs of the SXT/R391 family, given its conservation.

***mobI* is required for SXT^{MO10}-mediated transfer of chromosomal DNA.** Mobilization of chromosomal DNA in an Hfr-like manner by SXT^{MO10} has been previously described (26). Commonly, antibiotic resistance-conferring transposons located at defined positions in the *E. coli* genome are used as a selectable marker in Hfr mating experiments to monitor their mobilization and subsequent integration into the recipient chromosome by homologous recombination (27, 46). We took advantage of this ability to study whether *mobI* could be involved in the transfer of chromosomal DNA mediated by SXT^{MO10}.

In *E. coli* CAG18420, Tn*10kan* is inserted into *lacI* (7.9 min), which is located downstream from *prfC* (99.3 min), the integration site of SXT^{MO10} (27, 46). SXT^{MO10} has been shown to mobilize in *cis* the chromosomal locus *lacI*::Tn*10kan* at a frequency of 10^{-7} (27). Since deletion of *mobI* abolished transfer of SXT^{MO10}, we expected that this mutation would also abolish transfer of chromosomal DNA. We used *E. coli* CAG18420 SXT^{MO10} (VB82) and CAG18420 SXT^{MO10} Δ*mobI* (VB154) as donor strains in mating experiments to compare the frequency of mobilization of the chromosomal marker *lacI*::Tn*10kan.* As expected, deletion of *mobI* markedly reduced the transfer of *lacI*::Tn*10kan* (Fig. 5). Complementation of Δ*mobI* with pMobI-D restored transfer of this chromosomal marker to nearly wild-type levels (Fig. 5), and again, complementation with pMobI-B resulted in a weak restoration of mobilization of *lacI*::Tn*10kan*. Since SXT^{MO10}-mediated mobilization of *lacI*::Tn*10kan* was driven from $oriT_{SXT}$, the experiment described above did not allow us to determine whether *mobI* was involved in *oriT* recognition or mating pair formation; yet it emphasized the importance of *mobI* for conjugative transfer processes mediated by SXT^{MO10}.

***mobI* is not required for SXT^{MO10}-mediated transfer of CloDF13.** To investigate whether *mobI* functions in mating pair formation or in DNA processing, we took advantage of the ability of SXT^{MO10} to mobilize in *trans* plasmids such as the broad-host-range mobilizable plasmid CloDF13 (27). CloDF13 encodes its own mobilization proteins that recognize and act at its cognate *oriT* locus (13). We expected that if *mobI* was involved in

mating pair formation, the Δ*mobI* mutation would affect both the transfer of SXT^{MO10} and the mobilization of CloDF13. We transformed the wild-type SXT^{MO10} (VB82) and the SXT^{MO10} Δ*mobI* (VB154) *E. coli* strains with pSU4628, an Ap-resistant derivative of plasmid CloDF13 (Table 1), and used these strains as donors in mating experiments (Fig. 5).

Interestingly, the Δ*mobI* mutation did not abolish the mobilization in *trans* of pSU4628 (Fig. 5), highlighting the independence of pSU4628 transfer from SXT^{MO10}-encoded *mobI*. This observation strongly suggests that *mobI* encodes a protein that specifically recognizes SXT^{MO10} DNA, likely acting at *oriT*$_{SXT}$ but not playing any role in the formation of a functional mating bridge. On the contrary, the presence of *mobI* in the donor cells seemed to impair the transfer of CloDF13 since we observed that the rate of transfer of pSU4628 was about 2 orders of magnitude higher when mobilization was mediated by SXT^{MO10} Δ*mobI* than when it was mediated by wild-type SXT^{MO10} (Fig. 5). Since CloDF13 encodes its own mobilization proteins, we speculate that *mobI* competes with CloDF13-encoded activity or that transfer-proficient SXT^{MO10} and CloDF13 compete for the mating bridge when both are present in the same cell. This hypothesis is reinforced by the slight reductions of transfer of SXT^{MO10} and *lacI*::Tn*10kan* observed when pSU4628 was present in the wild-type donor strain (Fig. 5), as already described by Hochhut et al. (27).

DISCUSSION

Besides generating genetic diversity (20), conjugation is the major mechanism involved in the dissemination of antibiotic resistance (35). Despite the importance of the SXT/R391 family in the dissemination of antibiotic resistance among clinically important pathogens, such as *V. cholerae*, our knowledge of the genetic determinants required for initiation and termination of the conjugative transfer of this family of ICEs is still very limited (7). Here, we have defined a fundamental property of this family, the origin of transfer. We corrected a previous study (4) and found that the SXT^{MO10} *oriT* locus is contained in a 918-bp intergenic region located between s003 and *rumB′*. A 299-bp fragment internal to the 918-bp region was sufficient to allow mobilization of a low-copy-number, nonmobilizable plasmid by a mutant of SXT^{MO10} deficient for excision and integration. In fact, our observations indicate that this 299-bp fragment corresponds to the *oriT* loci of SXT^{MO10}, R391, R997, pMERPH, and very likely several if not all of the other ICEs of the SXT/R391 family.

Our findings contradict a previous report which suggested that *oriT*$_{SXT}$ was located within a 550-bp intergenic region located between *traD* and *traJ* (4). Beaber et al. reported that this fragment was sufficient to enable the mobilization by SXT^{MO10} of the high-copy-number, nonmobilizable vector pCR2.1 (4). However, Beaber et al. did not demonstrate that the mobility of this plasmid was independent of SXT^{MO10} transfer. Homologous recombination between SXT^{MO10} and the cloned fragment could have led to the cointegration of SXT^{MO10} with the plasmid and its subsequent mobilization to the recipient. In our hands, the 550-bp *traD-traJ* intergenic fragment did not enable mobilization of a low-copy-number, nonmobilizable vector by the excision-deficient SXT^{MO10}, whereas a 299-bp segment internal to the s003-*rumB′* fragment did so. Moreover, deletion of most of this region from SXT^{MO10} nearly abolished its transmissibility without altering the mobilization of a plasmid containing the 299-bp segment, underscoring the importance of this sequence as a *cis*-acting element necessary for transfer and mobilization.

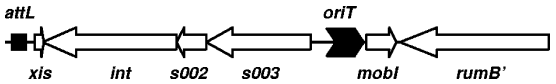

FIG. 6. Schematic representation of the *oriT* locus and surrounding genes. The arrow representing the *oriT* locus indicates the polarity of transfer as reported in Hochhut et al. (27).

Beaber et al. (3) previously reported that the genes and sequences encoding the conjugative machinery of SXT^{MO10} and R391 were divided in four functional clusters separated by ICE-specific insertions: the DNA-processing cluster *traID-oriT-traJ* and the three mating pore formation clusters *traLE KBVA*, *traC-trsF-traWUN*, and *traFHG*. The true origin of transfer is located upstream from s003 and the promoter that likely drives the expression of the integrase and upstream from *mobI*, a previously unannotated gene that is necessary for transfer of SXT^{MO10} (Fig. 6). We showed that *mobI* is required for mobilization of a nonmobilizable plasmid harboring *oriT*$_{SXT}$. Since this gene is not required for SXT^{MO10}-mediated mobilization of the broad-host-range mobilizable plasmid CloDF13, we suggest that it specifically recognizes and acts at the *oriT* loci of the ICEs of the SXT/R391 family. The absence of proteins homologous to the putative MobI protein in the GenBank database suggests that MobI belongs to a new class of mobilization proteins. Therefore, the DNA-processing functions are themselves divided in two clusters in the SXT/R391 family, the *traID*-VchoM_02001241-*traJ* cluster and the *oriT-mobI* cluster. The gene *mobI* is orientated in the same direction as all the other *tra* genes. This organization likely reflects an ancestral structure where all these genes were organized as an operon, later disrupted by insertions of foreign DNA (3, 9, 38, 40).

The locations of *oriT* and *mobI* within SXT^{MO10} likely have functional consequences. They are found directly upstream from the putative promoter region driving the expression of the genes s003, s002, and *int*, which are likely organized as an operon. s002 and s003 encode proteins of unknown functions, and *int* encodes the tyrosine recombinase Int (integrase) that catalyzes the integration and excision of the SXT/R391 ICEs (10, 28). A previous report described a functional interaction between the integrase Int$_{Tn916}$ and *oriT*$_{Tn916}$ of the conjugative transposon Tn*916* (25). Int$_{Tn916}$ binds specifically to *oriT*$_{Tn916}$, providing stability to the relaxase-DNA complex (45). The location of *oriT*$_{SXT}$ could reflect a possible role for Int in the regulation of excision and transfer of the ICE. For instance, similar to what was found for Tn*916*, binding of Int to *oriT*$_{SXT}$ could serve as a signal indicating that Int has been produced and that SXT^{MO10} has likely excised and is ready for transfer. In this scenario, binding of Int to *oriT*$_{SXT}$ would prevent the premature transfer of the integrated ICE, restricting transfer of only intact copies of the element to the recipient cells. However, previously published data indicated that neither *int* nor s002 and s003 are required for SXT^{MO10}-mediated transfer of chromosomal markers (10, 27). We also showed here that

FIG. 7. Schematic representation of an SXT^{MO10}-R391 tandem array and possible corresponding hybrid formed by *oriT* recombination.

pMRA, which contains *oriT*$_{SXT}$, is mobilizable to the recipient by SXT^{MO10} Δ*int*, indicating that excision of the ICE, and therefore expression of Int, is not a requisite prior to initiation of transfer at *oriT*$_{SXT}$.

It is worth noting that according to the new position of *oriT* and the polarity of DNA transfer that has been discovered by Hochhut et al. (27), the first gene that enters into the recipient cell is *mobI*, followed by the *rumAB* operon, which encodes a functional polV-like Y-family polymerase (37) when *rumB′* is not disrupted by a cluster of antibiotic resistance genes as in SXT^{MO10} (Fig. 6). Similarly, the last genes that enter the recipient cell are *xis*, *int*, s002, and s003. Late transfer of *int* is remarkable as de novo expression of this gene has been found to be necessary in the recipient to promote the integration of the circular SXT^{MO10} molecule into the recipient's chromosome (28). Besides the requirement of *int*, little is known to date about the early steps leading to the establishment of SXT/R391 ICEs into the new host cell.

An important consequence of the new position of *oriT* in SXT/R391 ICEs is that previously published observations need to be reinterpreted. Hybrid ICEs, which appear to correspond to an assemblage of parts originating from different parental ICEs from the SXT/R391 family, can be detected in many clinical and environmental vibrios. ICE*Vch*Mex1 (9), ICE*Vch*Moz3 (47), ICE*Pda*Spa1 (38), and ICE*Vch*Lao1 (48) are examples of what appear to be naturally occurring hybrids. A possible mechanism of hybrid ICE formation in which hybrid ICEs would form by transfer to the recipient of a DNA strand initiated at the *oriT* locus of the ICE located at the 5′ end and terminated at the *oriT* locus of the ICE located at the 3′ end of a tandem array was proposed (11) (Fig. 7). The region located between the *oriT*s of two ICEs integrated in a tandem fashion resembles and mimics the structure of the circular intermediate that serves as a substrate for transfer. Our observations indicate that such a mechanism would in fact be possible since we found that there is no barrier preventing the cross-recognition by the SXT/R391 ICEs of the *oriT* loci of other ICEs of the same family. However, the location of *oriT* so close to one of the borders of these ICEs likely limits the impact of such a mechanism of recombination on the diversity of the family and solely do not explain the variety of hybrid ICEs found in nature.

While prior characterizations of numerous *oriT*s of conjugative plasmids in both gram-positive and gram-negative bacteria have been made, *oriT*s of ICEs are not as well known or studied. To date, only two of them have been defined: the *oriT* locus of the conjugative transposon Tn*916* from *Enterococcus faecalis* and the *oriT* locus of ICE*Bs1* from *Bacillus subtilis* (30, 31). Now that the *oriT* locus of the SXT/R391 family of ICEs has been identified, many aspects of the mechanism that initiate and terminate the strand transfer remain to be discovered, especially the role of *mobI* in these phenomena. Characterization of the interactions between the proteins MobI and TraI and the *oriT* sequence are ongoing.

ACKNOWLEDGMENTS

We thank Matthew K. Waldor for the kind gift of many strains and critical reading of the manuscript. We are also grateful to Tony Pembroke for providing R997 and pMERPH. We acknowledge Joeli Marrero for helpful discussions.

This work was supported by a grant from the FQRNT new researcher start-up program. V.B. holds a Canada Research Chair in molecular biology (impact and evolution of bacterial mobile elements). D.C. holds a fellowship from the Cenci Bolognetti-Institut Pasteur Foundation, Italy.

REFERENCES

1. **Ahmed, A. M., S. Shinoda, and T. Shimamoto.** 2005. A variant type of *Vibrio cholerae* SXT element in a multidrug-resistant strain of *Vibrio fluvialis*. FEMS Microbiol. Lett. **242:**241–247.
2. **Altschul, S. F., W. Gish, W. Miller, E. W. Myers, and D. J. Lipman.** 1990. Basic local alignment search tool. J. Mol. Biol. **215:**403–410.
3. **Beaber, J. W., V. Burrus, B. Hochhut, and M. K. Waldor.** 2002. Comparison of SXT and R391, two conjugative integrating elements: definition of a genetic backbone for the mobilization of resistance determinants. Cell. Mol. Life Sci. **59:**2065–2070.
4. **Beaber, J. W., B. Hochhut, and M. K. Waldor.** 2002. Genomic and functional analyses of SXT, an integrating antibiotic resistance gene transfer element derived from *Vibrio cholerae*. J. Bacteriol. **184:**4259–4269.
5. **Beaber, J. W., B. Hochhut, and M. K. Waldor.** 2004. SOS response promotes horizontal dissemination of antibiotic resistance genes. Nature **427:**72–74.
6. **Böltner, D., C. MacMahon, J. T. Pembroke, P. Strike, and A. M. Osborn.** 2002. R391: a conjugative integrating mosaic comprised of phage, plasmid, and transposon elements. J. Bacteriol. **184:**5158–5169.
7. **Burrus, V., J. Marrero, and M. K. Waldor.** 2006. The current ICE age: biology and evolution of SXT-related integrating conjugative elements. Plasmid **55:**173–183.
8. **Burrus, V., G. Pavlovic, B. Decaris, and G. Guedon.** 2002. Conjugative transposons: the tip of the iceberg. Mol. Microbiol. **46:**601–610.
9. **Burrus, V., R. Quezada-Calvillo, J. Marrero, and M. K. Waldor.** 2006. SXT-related integrating conjugative element in New World *Vibrio cholerae*. Appl. Environ. Microbiol. **72:**3054–3057.
10. **Burrus, V., and M. K. Waldor.** 2003. Control of SXT integration and excision. J. Bacteriol. **185:**5045–5054.
11. **Burrus, V., and M. K. Waldor.** 2004. Formation of SXT tandem arrays and SXT-R391 hybrids. J. Bacteriol. **186:**2636–2645.
12. **Burrus, V., and M. K. Waldor.** 2004. Shaping bacterial genomes with integrative and conjugative elements. Res. Microbiol. **155:**376–386.
13. **Cabezon, E., J. I. Sastre, and F. de la Cruz.** 1997. Genetic evidence of a coupling role for the TraG protein family in bacterial conjugation. Mol. Gen. Genet. **254:**400–406.
14. **César, C. E., and M. Llosa.** 2007. TrwC-mediated site-specific recombination is controlled by host factors altering local DNA topology. J. Bacteriol. **189:**9037–9043.
15. **Chen, I., P. J. Christie, and D. Dubnau.** 2005. The ins and outs of DNA transfer in bacteria. Science **310:**1456–1460.
16. **Coetzee, J. N., N. Datta, and R. W. Hedges.** 1972. R factors from *Proteus rettgeri*. J. Gen. Microbiol. **72:**543–552.
17. **Datsenko, K. A., and B. L. Wanner.** 2000. One-step inactivation of chromosomal genes in *Escherichia coli* K-12 using PCR products. Proc. Natl. Acad. Sci. USA **97:**6640–6645.
18. **Dower, W. J., J. F. Miller, and C. W. Ragsdale.** 1988. High efficiency transformation of *E. coli* by high voltage electroporation. Nucleic Acids Res. **16:**6127–6145.
19. **Frost, L. S., K. Ippen-Ihler, and R. A. Skurray.** 1994. Analysis of the sequence and gene products of the transfer region of the F sex factor. Microbiol. Mol. Biol. Rev. **58:**162–210.
20. **Frost, L. S., R. Leplae, A. O. Summers, and A. Toussaint.** 2005. Mobile genetic elements: the agents of open source evolution. Nat. Rev. Microbiol. **3:**722–732.
21. **Furuya, N., and T. Komano.** 2000. Initiation and Termination of DNA transfer during conjugation of IncI1 plasmid R64: roles of two sets of inverted repeat sequences within *oriT* in termination of R64 transfer. J. Bacteriol. **182:**3191–3196.
22. **Grandoso, G., P. Avila, A. Cayon, M. A. Hernando, M. Llosa, and F. de la Cruz.** 2000. Two active-site tyrosyl residues of protein TrwC act sequentially at the origin of transfer during plasmid R388 conjugation. J. Mol. Biol. **295:**1163–1172.
23. **Grohmann, E., G. Muth, and M. Espinosa.** 2003. Conjugative plasmid transfer in gram-positive bacteria. Microbiol. Mol. Biol. Rev. **67:**277–301.

24. **Guasch, A., M. Lucas, G. Moncalian, M. Cabezas, R. Perez-Luque, F. X. Gomis-Ruth, F. de la Cruz, and M. Coll.** 2003. Recognition and processing of the origin of transfer DNA by conjugative relaxase TrwC. Nat. Struct. Biol. **10:**1002–1010.
25. **Hinerfeld, D., and G. Churchward.** 2001. Specific binding of integrase to the origin of transfer (*oriT*) of the conjugative transposon Tn*916*. J. Bacteriol. **183:**2947–2951.
26. **Hochhut, B., J. W. Beaber, R. Woodgate, and M. K. Waldor.** 2001. Formation of chromosomal tandem arrays of the SXT element and R391, two conjugative chromosomally integrating elements that share an attachment site. J. Bacteriol. **183:**1124–1132.
27. **Hochhut, B., J. Marrero, and M. K. Waldor.** 2000. Mobilization of plasmids and chromosomal DNA mediated by the SXT element, a constin found in *Vibrio cholerae* O139. J. Bacteriol. **182:**2043–2047.
28. **Hochhut, B., and M. K. Waldor.** 1999. Site-specific integration of the conjugal *Vibrio cholerae* SXT element into *prfC*. Mol. Microbiol. **32:**99–110.
29. **Iwanaga, M., C. Toma, T. Miyazato, S. Insisiengmay, N. Nakasone, and M. Ehara.** 2004. Antibiotic resistance conferred by a class I integron and SXT constin in *Vibrio cholerae* O1 strains isolated in Laos. Antimicrob. Agents Chemother. **48:**2364–2369.
30. **Jaworski, D. D., and D. B. Clewell.** 1995. A functional origin of transfer (*oriT*) on the conjugative transposon Tn*916*. J. Bacteriol. **177:**6644–6651.
31. **Lee, C. A., and A. D. Grossman.** 2007. Identification of the origin of transfer (*oriT*) and DNA relaxase required for conjugation of the integrative and conjugative element ICE*Bs1* of *Bacillus subtilis*. J. Bacteriol. **189:**7254–7261.
32. **Llosa, M., and F. de la Cruz.** 2005. Bacterial conjugation: a potential tool for genomic engineering. Res. Microbiol. **156:**1–6.
33. **Lukashin, A., and M. Borodovsky.** 1998. GeneMark.hmm: new solutions for gene finding. Nucleic Acids Res. **26:**1107–1115.
34. **Matson, S., and B. Morton.** 1991. *Escherichia coli* DNA helicase I catalyzes a site- and strand-specific nicking reaction at the F plasmid *oriT*. J. Biol. Chem. **266:**16232–16237.
35. **Mazel, D., and J. Davies.** 1999. Antibiotic resistance in microbes. Cell. Mol. Life Sci. **56:**742–754.
36. **McGrath, B. M., J. A. O'Halloran, and J. T. Pembroke.** 2005. Pre-exposure to UV irradiation increases the transfer frequency of the IncJ conjugative transposon-like elements R391, R392, R705, R706, R997 and pMERPH and is recA$^+$ dependent. FEMS Microbiol. Lett. **243:**461–465.
37. **Mead, S., A. Vaisman, M. Valjavec-Gratian, K. Karata, D. Vandewiele, and R. Woodgate.** 2007. Characterization of polVR391: a Y-family polymerase encoded by *rumA′B* from the IncJ conjugative transposon, R391. Mol. Microbiol. **63:**797–810.
38. **Osorio, C. R., J. Marrero, R. A. F. Wozniak, M. L. Lemos, V. Burrus, and M. K. Waldor.** 2008. Genomic and functional analysis of ICE*Pda*Spa1, a fish-pathogen-derived SXT-related integrating conjugative element that can mobilize a virulence plasmid. J. Bacteriol. **190:**3353–3361.
39. **Parker, C., E. Becker, X. Zhang, S. Jandle, and R. Meyer.** 2005. Elements in the co-evolution of relaxases and their origins of transfer. Plasmid **53:**113–118.
40. **Pembroke, J. T., and A. V. Piterina.** 2006. A novel ICE in the genome of *Shewanella putrefaciens* W3-18-1: comparison with the SXT/R391 ICE-like elements. FEMS Microbiol. Lett. **264:**80–88.
41. **Peters, S. E., J. L. Hobman, P. Strike, and D. A. Ritchie.** 1991. Novel mercury resistance determinants carried by IncJ plasmids pMERPH and R391. Mol. Gen. Genet. **228:**294–299.
42. **Ragonese, H., D. Haisch, E. Villareal, J.-H. Choi, and S. W. Matson.** 2007. The F plasmid-encoded TraM protein stimulates relaxosome-mediated cleavage at *oriT* through an interaction with TraI. Mol. Microbiol. **63:**1173–1184.
43. **Reygers, U., R. Wessel, H. Muller, and H. Hoffmann-Berling.** 1991. Endonuclease activity of *Escherichia coli* DNA helicase I directed against the transfer origin of the F factor. EMBO J. **10:**2689–2694.
44. **Rice, L. B.** 1998. Tn*916* family conjugative transposons and dissemination of antimicrobial resistance determinants. Antimicrob. Agents Chemother. **42:**1871–1877.
45. **Rocco, J. M., and G. Churchward.** 2006. The integrase of the conjugative transposon Tn*916* directs strand- and sequence-specific cleavage of the origin of conjugal transfer, *oriT*, by the endonuclease Orf20. J. Bacteriol. **188:**2207–2213.
46. **Singer, M., T. A. Baker, G. Schnitzler, S. M. Deischel, M. Goel, W. Dove, K. J. Jaacks, A. D. Grossman, J. W. Erickson, and C. A. Gross.** 1989. A collection of strains containing genetically linked alternating antibiotic resistance elements for genetic mapping of *Escherichia coli*. Microbiol. Rev. **53:**1–24.
47. **Taviani, E., D. Ceccarelli, N. Lazaro, S. Bani, P. Cappuccinelli, R. R. Colwell, and M. M. Colombo.** 2008. Environmental *Vibrio spp.*, isolated from Mozambique, contain a polymorphic group of integrative conjugative elements and class 1 integrons. FEMS Microbiol. Ecol. **64:**45–54.
48. **Toma, C., N. Nakasone, T. Song, and M. Iwanaga.** 2005. *Vibrio cholerae* SXT element, Laos. Emerg. Infect. Dis. **11:**346–347.
49. **Waldor, M. K., H. Tschape, and J. J. Mekalanos.** 1996. A new type of conjugative transposon encodes resistance to sulfamethoxazole, trimethoprim, and streptomycin in *Vibrio cholerae* O139. J. Bacteriol. **178:**4157–4165.
50. **Whittle, G., N. Shoemaker, and A. Salyers.** 2002. The role of *Bacteroides* conjugative transposons in the dissemination of antibiotic resistance genes. Cell. Mol. Life Sci. **59:**2044–2054.
51. **Williams, S. L., and J. F. Schildbach.** 2006. Examination of an inverted repeat within the F factor origin of transfer: context dependence of F TraI relaxase DNA specificity. Nucleic Acids Res. **34:**426–435.